the maximum disparity was still only 1.1% of the peak value, and the average deviation 0.4%. In fact it is likely that the deviations are more the fault of the quantum calculations than the classical, i.e., the neglect of contributions from $v' > 11$ and the use of a single J value in lieu of more complete rotational averaging. In any case it is clear that both treatments will generally be adequate for spectra of the type analyzed here. Similar agreement between classical and quantum spectra has been demonstrated previously for discrete transitions in Li_2 and Na_2.[9]

The contributions of the first four v' levels to the spectrum are shown in Figure 4. The structure is clearly of the reflection type, as expected for the monotonic difference potential.[27] Note also that discrete emission from low v' levels is negligible, as noted earlier.

Conclusion

The D' → (2332) $2_u(^3\Delta)$ transition in I_2 occurs as a broad band near 5050 Å in the emission spectrum in inert buffer gases and accounts for 8% of the total emission from the D' state. This band is analyzed by classical and quantum spectral simulations. The results indicate that the $2_u(^3\Delta)$ state may be bound by 300 cm^{-1}. For essentially structureless bound-free transitions like this one, classical and quantum methods yield virtually identical spectra.

The $2_u(^3\Delta)$ state becomes only the second of 10 which dissociate to I + I* to be experimentally characterized in any detail, although one of the $1u$ states has been identified through photofragment spectroscopy.[30] By contrast at least 7 of the 10 states arising from I + I have been identified. (A summary of these states and the known ion-air states may be found in ref 25.) The features in the 4600–4800-Å region of the emission spectrum have been interpreted as involving additional states near the I + I* limit, but this assignment remains tentative.[1] Theoretical calculations suggest that other states in this region may be appreciably bound.[31] Their experimental characterization remains a subject for future investigations.

Acknowledgment. This work was supported in part by the Air Force Office of Scientific Research.

Registry No. I_2, 7553-56-2.

(30) R. D. Clear and K. R. Wilson, *J. Mol. Spectrosc.*, **47**, 39 (1973).
(31) M. Saute and M. Aubert-Frecon, *J. Chem. Phys.*, **77**, 5639 (1982).

Characterization of p-Type CdTe Electrodes in Acetonitrile/Electrolyte Solutions. Nearly Ideal Behavior from Reductive Surface Pretreatments

Henry S. White, Antonio J. Ricco, and Mark S. Wrighton*

Department of Chemistry, Massachusetts Institute of Technology, Cambridge, Massachusetts 02139 *(Received: June 10, 1983; In Final Form: August 12, 1983)*

Single-crystal p-CdTe (E_g = 1.4 eV) electrodes have been characterized in CH_3CN/electrolyte solutions. Deliberate modification of the p-CdTe surface by etching in strongly oxidizing ($Cr_2O_7^{2-}/HNO_3$) or reducing ($S_2O_4^{2-}/OH^-$) solutions alters the p-CdTe surface to give rise to large differences in the electrochemical response in the dark and under illumination. The oxidative pretreatment apparently yields a p-CdTe surface that is Fermi level pinned, whereas the reductive pretreatment yields nearly ideal response. The pretreated electrodes were characterized by XPS, impedance measurements, and cyclic voltammetry in the presence of a number of reversible, one-electron redox couples. XPS indicates the presence of a Te-rich surface overlayer, composed of Te^0 and TeO_2, on CdTe etched in oxidizing media. Electrodes etched in reducing solutions yield XPS spectra nearly identical with those of an Ar-ion-sputtered CdTe sample, in terms of stoichiometry (1:1) and chemical state (Cd^{2+} and Te^{2-}) of cadmium and telluride. The differential capacitance of p-CdTe cathodes in CH_3CN/0.2 M [n-Bu_4N]BF_4 was measured in the dark over the potential range −0.2 to −1.0 V vs. SSCE. Linear Mott–Schottky plots ($E_{FB} \approx -0.4$ V vs. SSCE, $n_A \approx 2.5 \times 10^{15}$ cm^{-3}) are obtained for electrodes etched in $S_2O_4^{2-}/OH^-$ solutions consistent with ideal variation in the band bending as the electrode potential is varied. In contrast, p-CdTe etched in $Cr_2O_7^{2-}/HNO_3$ yields potential-independent values of differential capacitance, ~40–70 nF·cm^{-2}, consistent with constant band bending (<0.1 eV) over a wide potential range. Quasireversible cyclic voltammetry in the dark and negligible photovoltages under illumination are observed at p-CdTe electrodes pretreated with the oxidative etch, consistent with the small barrier height determined from capacitance measurements. The CdTe etched in $S_2O_4^{2-}/OH^-$ solution shows nearly ideal interfacial behavior. Photovoltages vary from 0.0 to 0.7 V for solution species having redox potentials from −0.4 to −2.0 V vs. SSCE. The sustained conversion of 632.8-nm light (~40 mW/cm^2) to electricity has been demonstrated to be ~8% efficient for a solution containing [1,2-dicyanobenzene]$^{0/-}$. The cell has an open-circuit photovoltage of up to 0.9 V, a short-circuit quantum yield for electron flow of ~0.5, and a fill factor of ~0.45.

An earlier report from this laboratory[1] demonstrated the ability to alter and control the photoelectrochemical response of n-type semiconducting CdTe by deliberate modification of the electrode surface. Specifically, the photovoltage, E_V, developed at CdTe photoanodes pretreated by chemical etching in strongly oxidizing solutions is found to be insensitive to the solution redox potential,[1,2] E_{redox}, over a large potential range. In contrast, electrodes etched by a reducing solution behave in an ideal fashion:[3]

(1) Tanaka, S.; Bruce, J. A.; Wrighton, M. S. *J. Phys. Chem.* **1981**, *85*, 3778.
(2) Aruchamy, A.; Wrighton, M. S. *J. Phys. Chem.* **1980**, *84*, 2848.
(3) Gerischer, H. In "Physical Chemistry: An Advanced Treatise"; Eyring, H.; Henderson, D.; Jost, W., Ed.; Academic Press: New York, 1970; Vol. 9A.

0022-3654/83/2087-5140$01.50/0

Scheme I: Interface Energetics for a p-Type Semiconductor in Contact with an Electrolyte/Redox Couple/Solvent System in the Dark at Equilibrium and under Illumination with Intense, $>E_g$ Light at Open Circuit

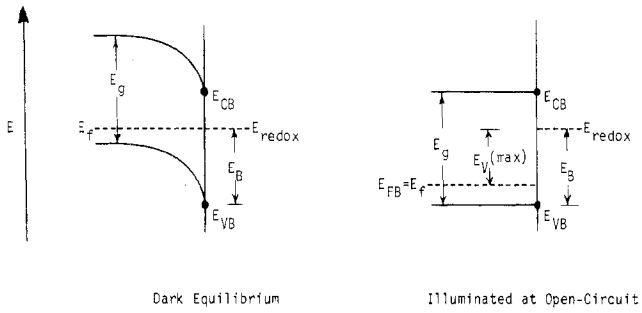

the observed E_V was found to increase linearly with more oxidizing solution potentials. We and others[1,2,4,5] generally assume that the maximum photovoltage, E_V(max), observed at a semiconductor electrode under illumination corresponds closely to the amount of band bending associated with the semiconductor/liquid electrolyte junction at equilibrium in the dark, Scheme I. The barrier height, E_B, is thus given by the value of E_V(max) plus the difference between the flat-band potential, E_{FB}, and the valence band position, E_{VB}. Thus, the constant photovoltage observed at "surface oxidized" n-CdTe electrodes indicates a constant barrier height, independent of the solution potential.[1] This situation is observed at small bandgap semiconductors[6] in contact with electrolytic solutions or metal overlayers and is referred to as "Fermi level pinning".[6] Fermi level pinning is associated with a high density of surface states located between the conduction and valence band edges E_{CB} and E_{VB}. Depending on the density and distribution of surface states, the charging of the surface states by equilibration of the surface redox species in solution or with the bulk of the semiconductor can result in a constant amount of band bending, independent of E_{redox}. In such cases variation in E_{redox} results in variation in the potential drop across the electrode/electrolyte interface (Helmholtz layer) and not across the semiconductor to cause changes in band bending. The large variation of photovoltage with E_{redox} observed at "surface reduced" n-type CdTe[1] leads to the conclusion that these surface energy levels can be removed by chemical methods, resulting in a more ideal CdTe semiconductor/liquid electrolyte junction.

We now wish to report the results of a related investigation concerning the influence of chemical pretreatment on the behavior of p-type CdTe in contact with CH_3CN/electrolyte solutions. In contrast to n-type cadmium chalcogenides,[7-10] CdX (X = S, Se, and Te), p-CdTe has been relatively unexplored as an electrode in photoelectrochemical cells. This is probably due, in part, to the poor performance found (E_V(max) ≤100 mV) in the few investigations.[11] We point out, however, that CdTe is one of the few II–VI compounds that can be made even moderately p-type[12] and that its bandgap, E_g, of 1.4 eV[13] corresponds to the optimum value for solar energy conversion.[14] Studies of p-CdTe/metal Schottky barriers have shown that it is possible to obtain relatively large values of E_B, but values of E_V(max) have apparently not been measured.[15] In view of the previous success from surface modification in altering the behavior of n-CdTe,[1] we felt that a similar strategy applied to p-type CdTe might result in an increase in its output performance. It is demonstrated that p-CdTe electrodes pretreated with a reducing etchant behave in a nearly ideal fashion with photovoltages varying from negligible values up to 0.9 V, depending on E_{redox}. In addition to measuring the photovoltage developed at illuminated electrodes, independent measurements of the barrier heights, E_B, of both oxidized and reduced p-type and n-type CdTe have been obtained from differential capacitance measurements. The values of E_B determined from capacitance studies correspond closely to the values determined from measuring E_V(max) of these materials, supporting the assumption that photovoltage is a reliable measure of the amount of band bending at equilibrium.

Experimental Section

Electrode Fabrication. Single crystals of p- and n-CdTe (Cleveland Crystals, Cleveland, OH) were cut into 0.05–0.2-cm^2 wafers approximately 1–2 mm thick. Before fabricating the crystals into electrodes, the side of the crystal to be exposed to the electrolyte solution was polished to a mirror finish with 0.3-μm alumina. Ohmic contact to n-CdTe was then made by rubbing In-Ga eutectic onto the back side of the crystal. Ohmic contact to p-CdTe was made by a slight modification of a procedure previously described by Aven and Garwacki for making ohmic contacts to p-ZnTe.[16] After the face to be exposed to solution was polished, the crystal was etched in boiling 5 M KOH for 1 min, rinsed thoroughly with H_2O, and dried. Approximately 20 $\mu L/cm^2$ of a 0.1 M $LiNO_3$ solution was applied to the back of the crystal and allowed to evaporate to dryness under an Ar atmosphere. The p-CdTe crystal was then heated slowly to 400 °C under a H_2–N_2 atmosphere (10% H_2) and held at this temperature for 1 h. Under these conditions Li is reported to diffuse slowly into the crystal. After cooling to room temperture, the crystal was rinsed with H_2O to remove excess $LiNO_3$, and a gold electroless contact was plated onto the Li diffused area with $HAuCl_4$. Excess plating solution was removed from the back surface with tissue and the contact was dried at 100 °C for ca. 2 min. A Cu wire was then attached to the ohmic contacts of both n- and p-CdTe by using Ag conducting paint and the entire assembly was mounted in glass tubing with ordinary epoxy leaving only the front crystal face, ⟨111⟩ orientation, exposed as previously described.[1]

Etching Procedure. CdTe electrodes were etched in reducing or oxidizing solutions immediately prior to their use. The oxidizing etch consisted of a 30-s immersion of the electrode in a solution containing 4 g of $K_2Cr_2O_7$, 10 mL of concentrated HNO_3, and 20 mL of H_2O. For the reducing etch, the electrode surface was initially oxidized in the above etchant, then immersed for 3 min in a boiling

(4) Gerischer, H. *J. Electroanal. Chem.* **1975**, *58*, 263.
(5) Frank, S. N.; Bard, A. J. *J. Am. Chem. Soc.* **1975**, *97*, 7427.
(6) Bard, A. J.; Bocarsly, A. B.; Fan, F.-R. F.; Walton, E. G.; Wrighton, M. S. *J. Am. Chem. Soc.* **1980**, *102*, 3671.
(7) Ellis, A. B.; Kaiser, S. W.; Wrighton, M. S. *J. Am. Chem. Soc.* **1976**, *98*, 1635.
(8) Ellis, A. B.; Bolts, J. M.; Wrighton, M. S. *J. Am. Chem. Soc.* **1977**, *99*, 2839, 2848, 4826.
(9) Hodes, G.; Manassen, J.; Cahen, D. *J. Appl. Electrochem.* **1977**, *7*, 181.
(10) Miller, B.; Heller, A. *Nature (London)* **1976**, *262*, 680.
(11) (a) Bockris, J. O'M.; Uosaki, K. *J. Electrochem. Soc.* **1977**, *124*, 1348. (b) Nadjo, L. *Ibid.* **1980**, *108*, 29. (c) Bolts, J. M.; Ellis, A. B.; Legg, K. D.; Wrighton, M. S. *J. Am. Chem. Soc.* **1977**, *99*, 4826.
(12) Crowder, B. L.; Hammer, W. N. *Phys. Rev.* **1966**, *150*, 541.
(13) Strauss, A. J. *Rev. Phys. Appl.* **1977**, *12*, 167.
(14) "American Physical Society Study Group on Photovoltaic Energy Conversion"; Ehrenreich H., Chairman; The American Physical Society: New York, 1979.
(15) Ponpon, J. P.; Saraphy, M.; Buttung, E.; Siffert, P. *Phys. Status Solidi* **1980**, *57*, 259.
(16) Aven, M.; Garwacki, W. *J. Electrochem. Soc.* **1967**, *114*, 1063.

solution of 0.6 M $Na_2S_2O_4$ and 2.5 M NaOH. After each etching the electrode was rinsed thoroughly with distilled H_2O, then acetone. Prolonged or repeated etching of CdTe electrodes resulted in a surface that appeared roughened; such electrodes showed poor, irreproducible electrochemical behavior and therefore were not employed until the surface had been repolished.

Electrochemical Procedure and Apparatus. Electrochemical measurements were made in a single compartment cell (~40 mL) equipped with an optically flat Pyrex window. Cyclic voltammetry was performed in Ar- or N_2-purged CH_3CN solutions containing 0.2 M [*n*-Bu_4N]-BF_4 as supporting electrolyte. The redox reagent concentration was typically 1–3 mM except where noted otherwise. Along with the semiconductor electrode, the cell contained a Pt disk electrode to check electrolyte and reagent purity, an 8-cm^2 Pt foil counterelectrode, and an aqueous sodium-saturated calomel reference electrode (SSCE). All potentials are reported vs. SSCE, which is 52-mV negative of the SCE (saturated calomel electrode).[17] Cyclic voltammograms were measured with a Pine Instruments Model RDE3 potentiostat/programmer and recorded on a Houston Instruments Model 2000 X–Y recorder.

Differential capacitance measurements were made under the conditions described above by employing a Princeton Applied Research Model 5204 lock-in amplifier with internal oscillator. Differential capacitance was recorded as a function of applied potential by scanning the d.c. potential at 5 mV/s. A ~10-mV peak-to-peak sine wave, 100 Hz–3 kHz, was used to modulate the electrode potential. Capacitance values were extracted from the quadrature values by assuming a simple *RC* series circuit. A dummy *RC* circuit was used to calibrate the measuring system. Quadrature readings were insensitive to *R* over the range 100–800 Ω, indicating a strict proportionality of the quadrature output to the actual capacitance value.

The light source used to irradiate the photoelectrodes was a beam-expanded 5-mW He–Ne laser (632.8 nm). Intensities were varied with a beam expander or by neutral density filters. A Tektronix J16 radiometer equipped with a J6502 probe was used to measure the input 632.8-nm optical power.

Photoaction Spectroscopy. Photoaction spectra were obtained by interfacing a PAR Model 6001 photoacoustic spectrometer with a potentiostat. The photoacoustic sample cell was replaced by a single-compartment three-electrode electrochemical cell with CdTe photoelectrode positioned in the light beam. While maintaining the photoelectrode on the plateau of the appropriate current–voltage curve, the wavelength was scanned and the output of the potentiostat sent to the Model 6001's microprocessor. A beam splitter and pyroelectric detector provided correction for variation in light intensity with wavelength, hence division of the resulting photocurrent spectra by a signal proportional to wavelength yielded relative quantum yield spectra. A 1-kW Xe arc lamp, modulated at 100 Hz, provided 10–100 mW/cm^2 of monochromatic visible light (8-nm resolution) to the photoelectrode. Lock-in detection eliminated dark current.

Surface Spectroscopy. X-ray photoelectron spectra were recorded on a PDP 11/04-controlled Physical Electronics (Perkin-Elmer) Model 548 spectrometer[18] equipped with Mg anode and cylindrical mirror analyzer (CMA). Spectra were recorded in digital format with a 0.5-eV step size and 100-eV pass energy for survey scans (1000–0 eV), and a 0.2-eV step size and 25-eV pass energy for multiplexes (10–20 eV windows about selected elemental lines). After removal of X-ray satellites, background subtraction, and correction for inelastic scattering, spectra were fit to Gaussian–Lorentzian line shapes to determine center, full width at half-maximum (fwhm), and integrated area of each peak. All binding energies were referenced to adventitious carbon, C 1s = 284.80 eV; the spectrometer work function was set with the Au $4f_{7/2}$ line (84.0 eV) and the linearity of the energy scale calibrated with the Cu $2p_{3/2}$, Cu Auger, and Cu 3p lines.[19] Binding energy corrections were normally <0.2 eV because all samples were conductors and were grounded to the spectrometer either by means of the Cu wire from the back contacts of photoelectrodes or by mounting crystals with conducting graphite paint. Sputter-cleaned surfaces were obtained with a 5-keV Ar ion beam, ~100 μA/cm^2, rastered over a 3 × 3 mm area, for 5 min.

Chemicals. HPLC grade CH_3CN (Baker) was purified and dried by distillation from P_2O_5 and stored over 4-Å molecular sieves. Tetrabutylammonium tetrafluoroborate was obtained from Southwestern Analytical Co. (Austin, TX) and dried at 70 °C for at least 24 h. Redox reagents employed in this investigation were either obtained commercially or synthesized by standard techniques. Their preparation and/or purification have been reported elsewhere.[20] The 1,2-dicyanobenzene was recrystallized from hot toluene. All other reagents were used without purification.

Results and Discussion

Cyclic Voltammetry of Various Redox Couples at p-CdTe The cyclic voltammetry of a number of redox species at reduced and oxidized p-CdTe was examined in order to determine the influence of surface etching procedures on the semiconductor/electrolyte interface. In particular, we have employed redox couples that show reversible, one-electron reductions at Pt in dry CH_3CN solutions containing 0.2 M [*n*-Bu_4N]BF_4 as supporting electrolyte. In the absence of any specific interactions between the redox species of interest and p-CdTe (such as strong adsorption), the resulting electrochemical behavior in the dark and under illumination should be dominated by the semiconductor/electrolyte energetics and not by kinetic limitations. No specific interactions between p-CdTe (reduced or oxidized) and the redox couples employed here were discerned in this investigation or in previous studies concerning n-CdTe.[1]

Cyclic voltammetry is commonly employed to measure the photovoltages developed at illuminated semiconductor electrodes immersed in electrolyte/redox couple solutions.[21,22] The potential difference between the voltammetric wave at a reversible electrode (such as Pt) and that observed at the illuminated semiconductor represents, to a close degree, the photovoltage developed under illumi-

(17) Bard, A. J.; Faulkner, L. R. In "Electrochemical Methods, Fundamentals and Applications"; Wiley: New York, 1980.

(18) The software for computer control of the XPS spectrometer, as well as data acquisition and curve fitting, is part of the MACS (Version VI) software package: Physical Electronics Division, Perkin-Elmer Corp., Eden Prairie, MN.

(19) Wagner, C. D. "Energy Calibration of Electron Spectrometer"; Barr, T. L.; Davis, L. E., Ed.; American Society for Testing and Materials, Applied Surface Analysis, ASTM STP 699; 1980, pp 137–47.

(20) (a) Schneemeyer, L. F.; Wrighton, M. S. *J. Am. Chem. Soc.* **1980**, *102*, 6964. (b) *Ibid.* **1979**, *101*, 6496. (c) Borcarsly, A. B.; Bookbinder, D. C.; Dominey, R. N.; Lewis, N. S.; Wrighton, M. S. *Ibid.* **1980**, *102*, 3683.

(21) Kautek, W.; Gerischer, H. *Ber. Bunsenges. Phys. Chem.* **1980**, *84*, 645. White, H. S.; Fan, F.-R. F.; Bard, A. J. *J. Electrochem. Soc.* **1981**, *128*, 1045. Kohl, P. A.; Bard, A. J. *J. Am. Chem. Soc.* **1977**, *99*, 7531.

(22) Baglio, J. A.; Calabrese, G. S.; Harrison, D. J.; Kamieniecki, E.; Ricco, A. J.; Wrighton, M. S.; Zoski, G. D. *J. Am. Chem. Soc.* **1983**, *105*, 2246, and references therein.

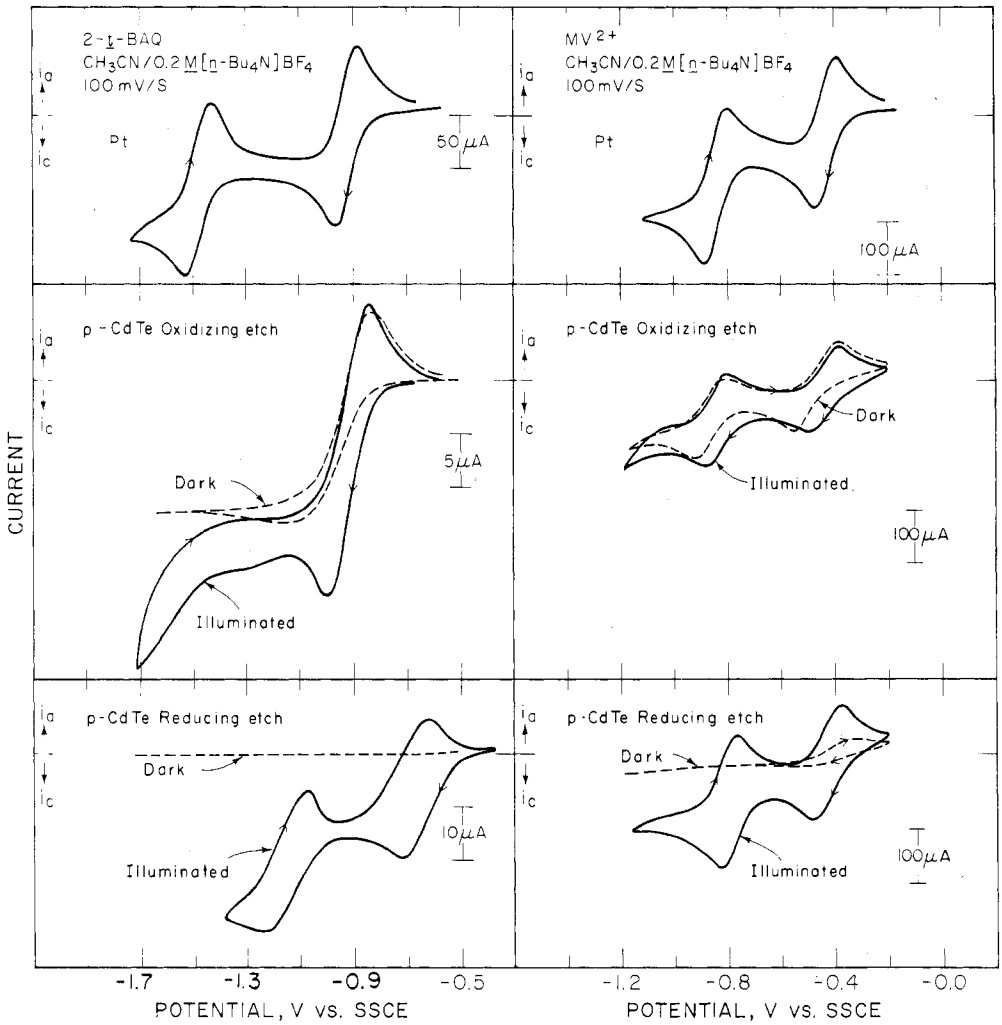

Figure 1. Comparison of cyclic voltammetry of 2-*tert*-butylanthraquinone, 2-t-BAQ, and *N*,*N*′-dimethyl-4,4′-bipyridinium, MV^{2+}, at Pt with surface "oxidized" and "reduced" p-CdTe (illuminated, —; dark, ----). Irradiation was at 632.8 nm, ~40 mW/cm^2.

nation. When only one-half of the redox couple is present in solution, we have found that the difference in potential of cathodic peak current observed at Pt, $E_{pc,Pt}$, and the semiconductor electrode, $E_{pc,CdTe}$, yields satisfactory E_V values consistent with the true open-circuit photovoltage measurable when both halves of the redox couple are present. Thus, photovoltages reported herein are given by eq 1. All values of $E_{pc,CdTe}$, and thus E_V, are the average

$$E_V = |E_{pc,p\text{-}CdTe} - E_{pc,Pt}| \quad (1)$$

values for a number of measurements at different p-CdTe electrodes and the estimated error in these values is ±0.1 V. The light intensity employed was ~40 mW/cm^2 for illuminated p-CdTe.

Figure 1 illustrates the differences between the electrochemical behavior of p-CdTe electrodes etched in the oxidizing etchant and those etched in the reducing etchant, when immersed in an electrolyte solution containing either 2-*tert*-butylanthraquinone (BAQ) or *N*,*N*′-dimethyl-4,4′-bipyridinium, MV^{2+}, at ~2 mM. Both electroactive species show two, well-resolved, one-electron reductions at Pt electrodes. The electrochemical response in the dark for the first and second reductions of MV^{2+} and for the first reduction of BAQ is typical of the behavior observed at "oxidized" p-CdTe electrodes for redox couples with redox potentials positive of ~−1.0 V vs. SSCE. Nearly reversible one-electron waves for these couples are observed at potentials corresponding closely to the values at Pt. In contrast, the electrochemial behavior of these couples in the dark at "reduced" p-CdTe is remarkably different, showing negligible cathodic currents due to the reduction of the electroactive solution species. Only a small anodic current is observed at "reduced" p-CdTe for the oxidation of some residual MV^+ present in the solution. The photoresponse of "oxidized" and "reduced" p-CdTe electrodes in these solutions is also dissimilar as shown in Figure 1. Upon illumination with 632.8-nm light, only a small increase in current is observed at "oxidized" p-CdTe for those couples that showed nearly reversible (or "ohmic") behavior in the dark ($MV^{2+/+}$, $MV^{+/0}$, and $BAQ^{0/-}$). The second reduction of BAQ at "oxidized" p-CdTe is observed upon illumination at approximately the same potential as on Pt, but the voltammetric wave at the p-CdTe is not well resolved. Further, some of the current can be attributed to reduction of the CdTe surface, as revealed in cyclic voltammograms recorded in the absence of a redox couple. It is worth pointing out that the cathodic peaks for these couples at the illuminated "oxidized" electrode, $E_{pc,CdTe}$, occur at essentially the same potential as at Pt and, thus, the photovoltage, E_V, is negligible. Illumination of the "oxidized" p-CdTe appears to slightly increase the rate of charge transfer across the semiconductor/electrolyte junction without affecting the potential at which the peak reduction current occurs. Reductions at "reduced" p-CdTe electrodes do not occur in the dark, but can be readily effected when the electrode is irradiated. Figure 1 shows that the reductions of BAQ occur at significantly less negative potentials than at either

TABLE I: Results from Cyclic Voltammetry of Various Redox Couples at Reduced and Oxidized p-CdTe

			reduced p-CdTe			oxidized p-CdTe		
redox couple, no.[a]	$E_{1/2}$[b,c]	$E_{pc,Pt}$	$E_{pc,CdTe}$	E_V,[d] V	dark behavior[e]	$E_{pc,CdTe}$	E_V,[d] V	dark behavior[e]
$TCNQ^{0/-}$, 1	0.20	0.15			ohmic	0.11	0	ohmic
$TCNQ^{-/2-}$, 2	−0.35	−0.40	−0.52	0	rectifying	−0.46	0	ohmic
$MV^{2+/+}$, 3	−0.43	−0.47	−0.46	0.01	rectifying	−0.47	0	ohmic
$MV^{+/0}$, 4	−0.84	−0.89	−0.80	0.09	rectifying	−0.88	0.01	ohmic
$BAQ^{0/-}$, 5	−0.93	−0.97	−0.81	0.16	rectifying	−1.01	0	ohmic
$Ru(bpy)_3^{2+/+}$, 6	−1.32	−1.36	−0.98	0.38	rectifying	−1.30	0.06	ohmic
$BAQ^{-/2-}$, 7	−1.51	−1.60	−1.20	0.40	rectifying	*f*	*f*	rectifying
$Ru(bpy)_3^{+/0}$, 8	−1.52	−1.55	−1.11	0.44	rectifying	−1.64	0	ohmic
$1,2\text{-}DCB^{0/-}$, 9	−1.62	−1.68	−1.13	0.55	rectifying			
$Ru(bpy)_3^{0/-}$, 10	−1.77	−1.81	−1.21	0.60	rectifying	−1.82	0	ohmic
$An^{0/-}$, 11	−2.01	−2.06	−1.43	0.63	rectifying			

[a] All data are for CH_3CN/0.2 M $[n\text{-}Bu_4N]BF_4$ solutions at 25 °C. Scan rates are 5–100 mV/s. Redox reagent concentrations are 1–3 mM. TCNQ is tetracyanoquinodimethane; MV is *N,N'*-dimethyl-4,4'-bipyridinium; BAQ is 2-*tert*-butyl-9,10-anthraquinone; bpy is 2,2'-bipyridine; DCB is dicyanobenzene; and An is anthracene. The numbers after each redox couple refer to the data points in Figure 3. [b] All potentials referenced to SSCE. [c] $E_{1/2}$'s calculated from cyclic voltammetry data according to $E_{1/2} = (E_{pa} + E_{pc})/2$ where E_{pa} and E_{pc} refer to potentials of the anodic and cathodic peak current. [d] Cf. eq 1 of text. Illumination provided by a He-Ne laser (632.8 nm) at ~40 mW/cm². [e] "Ohmic" and "rectifying" refer to the presence and absence, respectively, of a well-defined cyclic voltammetric wave in the dark due to the reduction of the electroactive species. [f] No well-defined peak potential was observed for $BAQ^{-/2-}$ at illuminated p-CdTe (see Figure 1 and text).

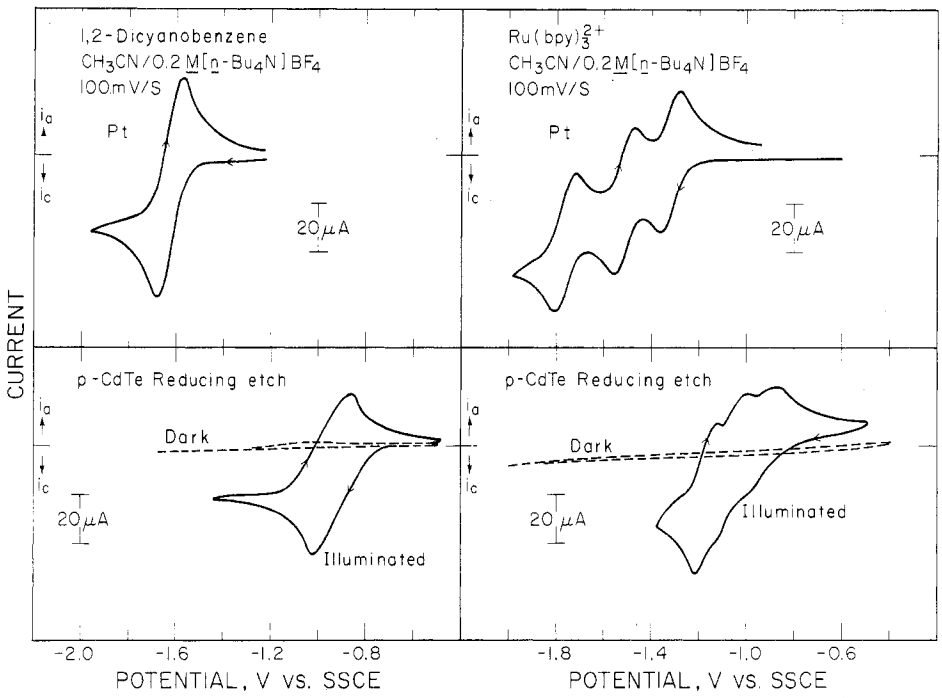

Figure 2. Comparison of cyclic voltammetry of $Ru(bpy)_3^{2+}$ and 1,2-dicyanobenzene at Pt with surface "reduced" p-CdTe (illuminated, —; dark, ----). Irradiation was at 632.8 nm, ~40 mW/cm².

"oxidized" p-CdTe or Pt. The difference in $E_{pc,Pt}$ and $E_{pc,CdTe(reduced)}$ is 0.16 and 0.31 V for the first and second BAQ reduction, respectively. Similarly, MV^{2+} can be effectively photoreduced at "reduced" p-CdTe, but with smaller E_V values. The first reduction occurs at potentials essentially identical with Pt ($E_V \simeq 0.01$), and only a modest photovoltage is observed for the second reduction ($E_V \simeq 0.09$ V). These results and those obtained in solutions containing other redox species are listed in Table I for "reduced" and "oxidized" p-CdTe electrodes.

Comparison of voltammetric results at "reduced" and "oxidized" p-CdTe for those electroactive species having redox potentials more negative than −1.5 V vs. SSCE is difficult, due to the electrochemical reduction of the "oxidized" p-CdTe surface which gives rise to large cathodic currents and irreproducible behavior. For instance, the initial cyclic voltammogram observed for "oxidized" p-CdTe in the presence of $Ru(bpy)_3^{2+}$ shows a broad cathodic wave extending from ~−1.2 to −2.0 V vs. SSCE; this same wave is observed in the absence of $Ru(bpy)_3^{2+}$ and is assigned to the reduction of a surface tellurium/tellurium oxide layer (see Surface Analysis, below). Repeated potential cycling of the "oxidized" p-CdTe electrode from −1.0 to −2.0 V vs. SSCE eventually (~10–15 scans) results in behavior resembling that observed for p-CdTe etched in the reducing etch: negligible dark current is observed in the potential region between ~−0.4 and −2.0 V vs. SSCE, and good photovoltages can be obtained for redox couples having $E_{1/2}$ more negative than ~−0.8 V vs SSCE. Small background photocurrents are observed at potentials more negative than ~−1.5 V when no redox couple is added. This photocurrent is possibly due to the reduction of CdTe,[23] resulting in the dissolution of the semiconductor. The response of $Ru(bpy)_3^{2+}$ and 1,2-di-

(23) Bard, A. J.; Wrighton, M. S. *J. Electrochem. Soc.* **1977**, *124*, 1706.

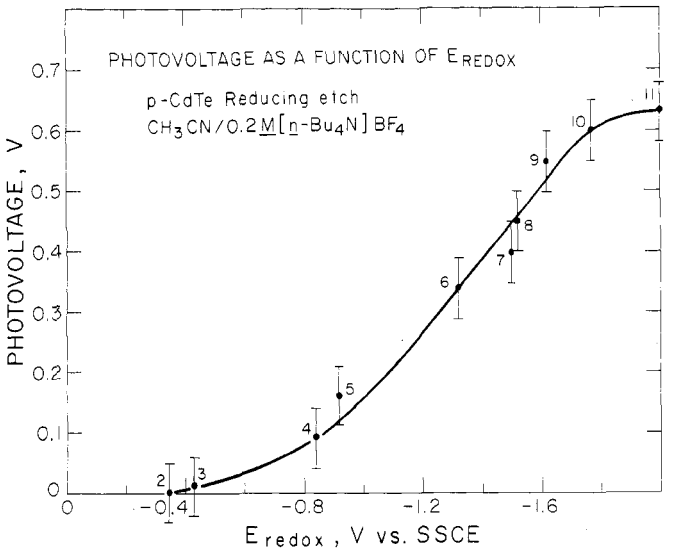

Figure 3. Plot of photovoltage at "reduced" p-CdTe as a function of E_{redox} for various redox couples. Redox couples are identified by number listed in Table I. Photovoltage is as defined in text, eq 2.

cyanobenzene at "reduced" p-CdTe in the dark and under illumination is shown in Figure 2. The reduction of $Ru(bpy)_3^{2+}$ at Pt shows three one-electron voltammetric waves that are well-separated (by ca. 200 mV). At illuminated "reduced" p-CdTe these three waves are significantly less resolved, showing peak separations of only 70 and 150 mV. In essence, the three reversible $Ru(bpy)_3^{2+}$ reductions, which occur at differing potentials at Pt are observed at nearly the same electrode potentials at illuminated p-CdTe, yielding E_V values of 0.38, 0.45, and 0.60 V, respectively. This behavior demonstrates nicely one of our conclusions regarding "reduced" p-CdTe: the barrier height and photovoltage depend largely on the redox potential of the contacting electrolyte solution. Photoreductions of electroactive species with quite negative potentials can also be affected at p-CdTe, as demonstrated for the case of 1,2-dicyanobenzene ($E_{1/2}$ = −1.62 V vs. SSCE). The E_V for this species at p-CdTe is 0.55 V by cyclic voltammetry at $S_2O_4^{2-}/OH^-$ treated electrodes. The electroactive species studied with the most negative reduction potential, anthracene ($E_{1/2} \cong$ −2.0 V vs. SSCE), also gave the largest photovoltage, E_V = 0.63 V, consistent with an E_{redox} dependent barrier height at the reduced surface.

Figure 3 shows the variation in photovoltage at "reduced" p-CdTe with changes in the electrochemical potential of the contacting electrolyte solution. Values of E_V for "oxidized" p-CdTe electrodes, which were not greater than 0.1 V for any redox couple examined (Table I), are not shown. Several conclusions can be drawn from mapping out the energetics of the semiconductor/electrolyte interface as in Figure 3. First, significant photovoltages are not observed for couples having redox potentials positive of −0.4 V. Thus, we take −0.4 V vs. SSCE to be approximately equal to the flat-band potential, E_{FB}, Scheme I. This is in good agreement with capacitance results (vide infra). The second conclusion drawn from Figure 3 is that the photovoltages, while increasing at more negative redox potentials, do not reach values expected for an ideal junction. The largest rate of increase of E_V, i.e., $\Delta E_V/\Delta E_{redox}$, is about 0.6, considerably less than the value of 1.0 predicted from eq 2. This nonideal behavior has

$$E_V = |E_{redox} - E_{FB}| \quad (2)$$

been observed before for other semiconductors[24] and is probably due to direct recombination of photogenerated charge carriers within the semiconductor interior or via interfacial states. Note that the correspondence between E_V and E_{redox} is not strictly linear (i.e., $\Delta E_V/\Delta E_{redox}$ is not constant over the entire range), indicating that recombination rates are potential dependent.

Differential Capacitance of p- and n-CdTe in CH_3CN/Electrolyte Solutions. The behavior of p-CdTe presented above and that reported earlier for n-CdTe[1] indicates that the barrier height associated with the semiconductor/electrolyte junction depends on the surface pretreatment. To gain further understanding of this phenomenon we have determined the space charge capacitance, C_{sc}, of these materials as a function of electrode potential, E_f, in CH_3CN containing only 0.2 M $[n\text{-}Bu_4N]BF_4$.[25] The differential capacitance has been taken to be equal to C_{sc} and has been measured as described in the Experimental Section. Results for both "oxidized" and "reduced" p- and n-CdTe are shown in Figure 4, along with the resulting Mott–Schottky data ($1/C_{sc}^2$ vs. E_f). These figures show typical results of a number of measurements on independently prepared CdTe electrodes. The C_{sc} vs. E_f data for "reduced" n- and p-CdTe are consistent with a variation in the band bending as the electrode potential is varied resulting in a strong variation in C_{sc}. In contrast, C_{sc} values for CdTe electrodes etched in the oxidizing etchant are virtually independent of E_f indicating that the space charge, and thus band bending, remains constant over a wide potential range.

The general shape and magnitude of the $1/C_{sc}^2$ vs. E_f plots were found to be independent of the modulation frequency between 100 and 3000 Hz. However, significant differences in C_{sc} values were observed, even at a fixed frequency, between repetitive measurements leading to scatter in the values of intercept (±0.1 V) and slope (±20%) of the Mott–Schottky plots. This somewhat erratic behavior is due to changes in the chemical composition of the surface upon cycling the electrode potential between negative and positive values. So that this could be demonstrated more clearly, an "oxidized" n-type CdTe electrode, which yielded a potential-independent C_{sc} value (~80 nF/cm^2), was potentiostatted at −1.8 V vs. SSCE for 15 min in the dark. At this potential the differential capacitance immediately begins to increase and reaches a limiting value (~700 nF/cm^2) after 10 min, equal to within 5% of the differential capacitance of the same electrode etched in the reducing etchant. Furthermore, the Mott-Schottky plot obtained after electrochemical reduction of the surface in the dark was similar to that obtained after chemical reduction. Because of this chemical instability of the CdTe surfaces we have not attempted systematic investigation of the frequency dependence of the capacitance. The effect of the negative electrode potential on the value of C_{sc} vs. E_f, however, does accord well with the photovoltage measurements described above where electrochemical reduction of "oxidized" p-CdTe ultimately yields good photovoltages.

The capacitance of an ideal semiconductor/electrolyte junction should obey the Mott–Schottky relationship, eq 3, at potentials where a depletion layer is formed.[25] In eq

$$[C_{sc}]^{-2} = 2(-E_B - kT/e)/n\epsilon\epsilon_0 e \quad (3)$$

3 n is the donor (n-type) or acceptor (p-type) density; ϵ is the semiconductor dielectric constant; ϵ_0 is the permittivity

(24) Fan, F.-R. F.; White, H. S.; Wheeler, B.; Bard, A. J. *J. Am. Chem. Soc.* **1980**, *102*, 5142.

(25) For a detailed description of the semiconductor/electrolyte junction capacitance, see Myamlin, V. A.; Pleskov, Y. V. In "Electrochemistry of Semiconductors"; Plenum Press: New York, 1967.

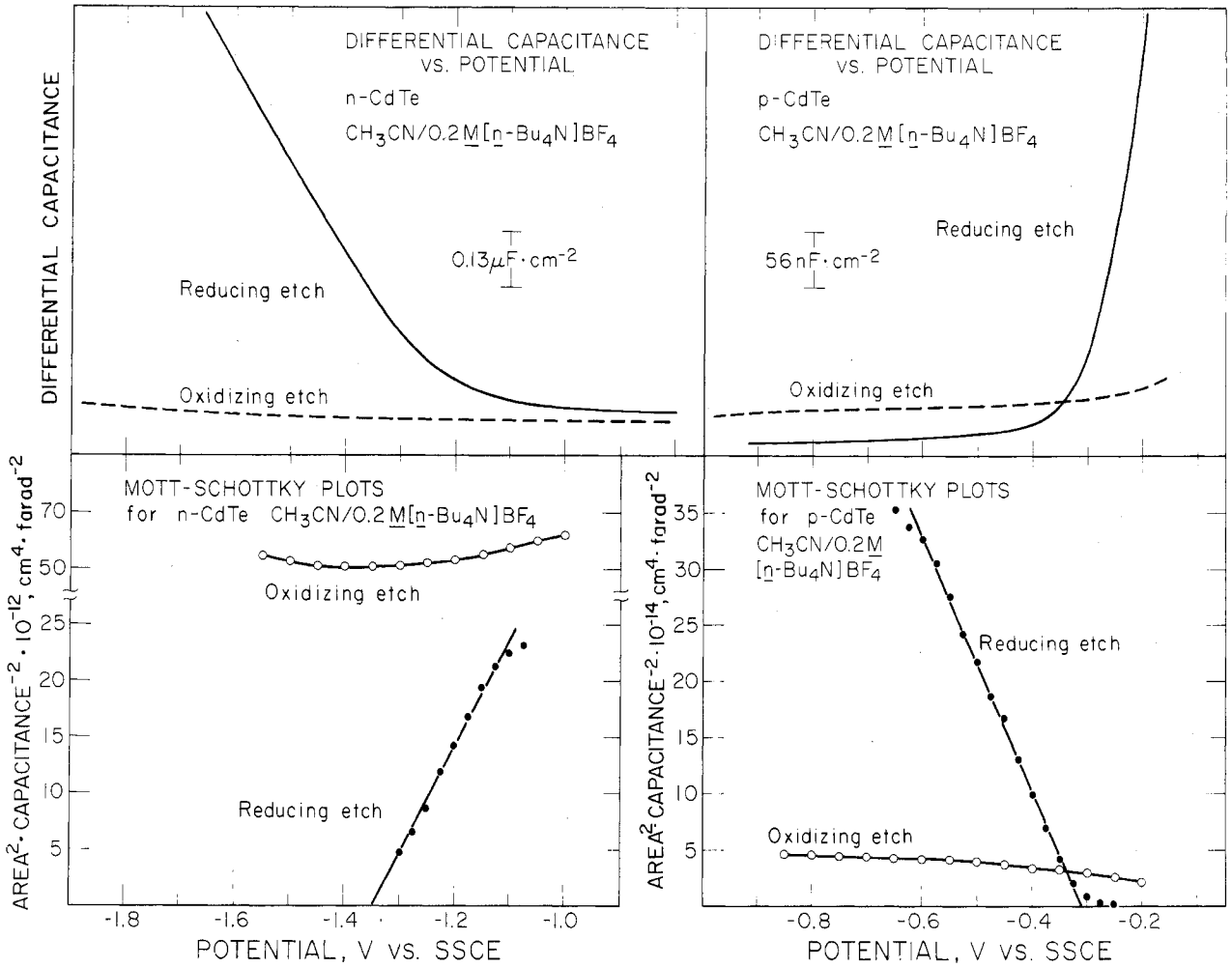

Figure 4. Comparison of differential capacitance and the resulting Mott–Schottky plots for surface oxidized (----) and reduced (—) p- and n-type CdTe at a modulation frequency of 1000 Hz.

constant; and e is the electronic charge. The literature value[26] of 7.2 for ϵ was used in all calculations. In the absence of a high density of surface states or deep donor levels a plot of $1/C_{sc}^2$ vs. E_f should be linear and have an extrapolated intercept equal to $\sim E_{FB}$ (the correction for kT/e being 27 mV at room temperature). Our plots of $1/C_{sc}^2$ vs. E_f, Figue 4, are linear for both "reduced" n- and p-CdTe in contact with $CH_3CN/[n\text{-}Bu_4N]BF_4$. The extrapolated intercepts (average values for a number of determinations) yield values of E_{FB} of −1.4 and −0.4 V vs. SSCE for n- and p-type electrodes, respectively. The donor (n-type) and acceptor (p-type) densities determined from the slopes of the Mott-Schottky plots are 2×10^{17} and 2.5×10^{15} cm^{-3}, respectively. These carrier densities allow a calculation of the separation of E_f from the top of the valence band or bottom of the conduction band in the bulk of p- or n-CdTe, respectively. For p-CdTe the valence band position, E_{VB}, can thus be calculated from eq 4 and 5[25] where N_v is the density of states and m_h^* is the effective

$$N_v = 2(2\pi m_h^* kT/h^2)^{3/2} \quad (4)$$

$$n_A/N_v = \exp(-(E_{VB} - E_{FB})/kT) \quad (5)$$

hole mass. Using $m_h^* = 0.35m_e$[27] (the electron rest mass) places E_{VB} at −0.2 V vs. SSCE. A similar calculation for n-CdTe places the conduction band, E_{CB}, at −1.5 V vs. SSCE.[28] The difference between E_{VB} and E_{CB}, 1.3 V, is within experimental error of the reported band gap, 1.4 V, of CdTe. The value of E_{FB} for the "reduced" n-CdTe is, within experimental error, the same value obtained from photovoltage measurements.[1]

Comparison of the $1/C_{sc}^2$ vs. E_f plots for "oxidized" and "reduced" CdTe electrodes yields quantitative information regarding the value of the potential-independent barrier height, E_B, resulting from the oxidizing etch. We can assume that when C_{sc} for "oxidized" n- or p-CdTe equals C_{sc} for "reduced" n- or p-CdTe the band bending is the same in the "oxidized" and "reduced" n- or p-CdTe. The amount of band bending is obtained by measuring the potential difference between E_{FB} (the intercept of the straight line drawn through $1/C_{sc}^2$ data for the "reduced" surface) and the potential at which the $1/C_{sc}^2$ values for both "oxidized" and "reduced" electrodes are equal. At this potential the band bending in both electrodes is the same and, since E_{FB} is fixed for the "reduced" sample, the band bending is thus measureable. From Figure 4 we observe that the difference between these two values for p-CdTe is equal to ~50 mV. Other determinations of the amount of band bending by this method for p-CdTe were in the range 5–80 mV, indicating that the band bending

(26) van Vechten, J. A. *Phys. Rev.* **1969**, *182*, 899.

(27) Values of 0.35 and 0.14 for the effective hole and electron mass of CdTe, respectively, were taken from the "Handbook of Chemistry and Physics"; Weast, R. C., Ed.; The Chemical Rubber Co.: Cleveland, OH, 1970–1971; Vol. 51. Slightly different values, 0.8 (m_h^*) and 0.10 (m_e^*) are given in ref 13. These differences do not appreciably change the value of E_{CB} or E_{VB} calculated with eq 4 and 5.

(28) In calculating the position of the conduction band edge, E_{CB}, m_e^* is substituted for m_h^* in eq 4 and $(E_{FB}-E_{CB})$ is substituted for $(E_{VB} - E_{FB})$ in eq 6.

TABLE II: Summary of XPS Data for Chemical State and Stoichiometry of Oxidized, Reduced, and Ion-Sputtered CdTe[a]

surface examined	signals observed, eV	rel int[b]	assignment	core level
sputtered CdTe	405.08 (6)	1.0	Cd^{2+}	$3d_{5/2}$
	411.84 (6)			$3d_{3/2}$
	572.47 (5)	1.1 (1)	Te^{2-}	$3d_{5/2}$
	582.87 (4)			$3d_{3/2}$
"reduced" CdTe	404.94 (7)	1.0	Cd^{2+}	$3d_{5/2}$
	411.69 (6)			$3d_{3/2}$
	572.50 (7)	1.0 (3)	Te^{2-}	$3d_{5/2}$
	582.92 (7)			$3d_{3/2}$
	575.96 (11)	0.04 (5)	TeO_2	$3d_{5/2}$
	586.27 (15)			$3d_{3/2}$
"oxidized" CdTe	405.15 (7)	1.0	Cd^{2+}	$3d_{5/2}$
	411.90 (8)			$3d_{3/2}$
	572.98 (11)	1.2 (1)	"mixed" Te^{2-}/Te^0	$3d_{5/2}$
	583.40 (11)			$3d_{3/2}$
	576.21 (10)	0.4 (2)	TeO_2	$3d_{5/2}$
	586.58 (10)			$3d_{3/2}$
air-oxidized Te	573.5	0.05	Te^0	$3d_{5/2}$
	583.8			$3d_{3/2}$
	576.4	1.0	TeO_2	$3d_{5/2}$
	586.8			$3d_{3/2}$
sputtered Te	573.54	1.0	Te^0	$3d_{5/2}$
	583.92			$3d_{3/2}$

[a] Each tabulated value for CdTe is the average of four to six runs. Uncertainty in the last digit of each entry, given parenthetically, is estimated as twice the standard deviation of the average. More extensive data are published elsewhere.[36] [b] Relative intensities are calculated from integrated peak areas of the curve fit data and are corrected for atomic sensitivity factors: Wagner, C. D.; Davis, L. E.; Zeller, M. V.; Taylor, J. A.; Raymond, R. H.; Gale, L. H. *Surf. Interface Anal.* 1981, *3*, 211.

at "oxidized" p–CdTe is very small. This is in good agreement with the cyclic voltammetry results for "oxidized" p-CdTe which show "ohmic" behavior in the dark and photovoltages less than 100 mV for a number of electroactive species, Table I. If we take $|E_{FB} - E_{VB}|$ to be ~0.2 V, from eq 4 and 5, this means that the value of E_B for "oxidized" p-CdTe is ~0.3 V. The band bending of "oxidized" n-CdTe samples, measured by the same procedure, is 0.5–0.7 V, a much larger value than with p-CdTe, in agreement with the observed photovoltage at such electrodes.[1,2] Thus, for "oxidized" n-CdTe the value of E_B is ~0.8 V.

The E_{redox}-independent barrier height of "oxidized" n- and p-CdTe indicates that the photovoltages developed at these electrodes are limited by Fermi level pinning and not by carrier inversion. This is unequivocal for p-CdTe where the small barrier height ($E_B \cong 0.3$ V) cannot be due to carrier inversion of a 1.4-eV band-gap semiconductor.[25] The constant C_{sc} value observed for n-CdTe, even at potentials extending 0.6-V negative of the conduction band edge (E_{CB} as measured from the Mott–Schottky plots of the "reduced" electrodes), also indicates that the band bending is limited by Fermi level pinning. Even if carrier inversion were important for "oxidized" n-CdTe it is necessary to conclude from Figure 4 that surface levels initially pin the Fermi level to a potential positive enough to create an accumulation of minority carriers at potentials negative of E_{CB}.

In related investigations,[29] the diffferential capacitance curves of p-Si in the presence of a number of redox couples show that Fermi level pinning controls the extent of band bending in that material. These results, however, are considerably different from the results reported here. The shape of the C_{sc} vs. E_f curve for p-Si is found to be independent of the contacting solution and closely resembles expectations for an ideal extrinsic p-type semiconductor (similar in shape to the capacitance–potential curve for "reduced" p-CdTe, Figure 4). However, it is found that the differential capacitance curves are shifted along the potential axis depending on the redox potential of the solution electroactive species. A linear relationship between E_{FB}, determined from the Mott-Schottky plots, and E_{redox} is observed over a considerable potential range. The p-Si in solvent/electrolyte solution containing no redox couple also gives a nearly ideal Mott–Schottky plot. The point is we conclude that "oxidized" CdTe is Fermi level pinned and yet the value of C_{sc} is invariant with changes in E_f. Changes in E_f for "oxidized" CdTe apparently give changes in the Helmholtz capacitance, not in C_{sc}. The difference in behavior of CdTe and p-Si can be understood by noting that accumulation of surface charge can occur by either of two mechanisms: (1) equilibration of the semiconductor bulk with its surface, i.e., electrons are driven to surface states of a p-type semiconductor creating a net negative surface charge or (2) equilibration of solution redox reagents with the semiconductor surface, i.e., electron transfer from a solution donor species to the surface states. The latter mechanism is apparently responsible for the behavior of p-Si and is consistent with a nonuniform and low density of surface states that are not able to exchange electrons with bulk p-Si. For CdTe there appears to be essentially a continuum of states between E_{VB} and E_{CB}, because the overlayer for the "oxidized" CdTe is Te^0 (vide infra), a small gap semiconductor. We attempted to measure C_{sc} in the presence of various redox couples. But leakage currents precluded meaningful results.

X-ray Photoelectron Spectroscopy of CdTe Surfaces. X-ray photoelectron spectroscopy of CdTe surfaces reveals substantial differences in surface composition of samples treated with the oxidizing vs. the reducing etch. Precise core electron binding energies were measured for the Cd $3d_{5/2,3/2}$, Te $3d_{5/2,3/2}$, and C 1s levels of each sample. A low-resolution survey scan was also taken to reveal impurities and to quantitate any oxide present. Table II summarizes XPS data obtained from the various samples; values given are the average of four to six runs. The similarity of the Cd 3d binding energies of oxidized, reduced,

(29) (a) Nagasubramanian, G.; Wheeler, B. L.; Fan, F.-R. F.; Bard, A. J. *J. Electrochem. Soc.* **1982**, *129*, 1743. (b) Kerita, B.; Kawenoki, I.; Kossanyi, J.; Garreau, D.; Nadjo, L. *Ibid.* **1983**, *145*, 293.

TABLE III: Efficiency for Photoreduction of 1,2-Dicyanobenzene at Illuminated p-CdTe in CH_3CN/0.2 M $[n\text{-}Bu_4N]BF_4$

electrode[a]	solution[b]	input pwr,[c] mW/cm²	E_V(oc),[d] V	Φ_e[e]	ff[f]	% η[g]
1	0.1 M 1,2-DCB (unpoised)	22	0.70	0.51	0.43	7.9
		11.6	0.70	0.56	0.44	8.6
		6.5	0.70	0.54	0.45	8.5
2	0.1 M 1,2-DCB (unpoised)	40.0	0.75	0.49	0.46	8.7
		20.0	0.74	0.51	0.50	9.5
		10.3	0.72	0.55	0.52	10.5
		5.2	0.70	0.54	0.54	10.4
3	0.1 M 1,2-DCB/2 mM 1,2-DCB⁻ (poised; $E_{redox} = -1.50$ V vs. SSCE)	38.7	0.92	0.48	0.28	6.2
		21.9	0.92	0.52	0.36	8.7
		6.1	0.90	0.51	0.44	10.3
		3.0	0.82	0.55	0.48	10.9

[a] 1, 2, and 3 refer to different electrodes. [b] Stirred and purged with Ar. [c] Input irradiation at 632.8 nm. [d] E_V(oc) is the open-circuit photovoltage. [e] Quantum yield for electron flow at E_{redox}. Data are uncorrected for reflection losses or losses from redox couple absorption. [f] Fill factor, defined by eq 6 in text. [g] Defined by eq 7 in text.

and sputtered samples indicates there is no major variation in the chemical state of Cd. In particular, none of the Cd 3d binding energies is characteristic of Cd^0 or CdO, ruling out these species as major surface constituents.[30] Substantial variation is found, however, in the Te 3d region, as illustrated in Figure 5 and indicated in Table II. In addition to altering the Te chemical state, the type of etch also affects surface stoichiometry, as summarized in Table II.

The Te 3d XPS data for CdTe treated with the oxidizing etch (Figure 5, top) reveals two sets of Te $3d_{5/2,3/2}$ bands split by ~3.2 eV. The higher binding energy set, several electronvolts higher than either Te^{2-} or Te^0 (as measured for sputtered CdTe and Te^0, respectively) is assigned to TeO_2, the lowest stable oxide of Te,[31] in agreement with assignments made elsewhere for the Te 3d levels of CdTe[32] cleaved in air and in agreement with the $3d_{5/2}$ binding energy reported for TeO_2 (575.9 eV).[33] The lower binding energy set of bands, lying midway between Te^0 and Te^{2-}, results from both Te^0 and underlying (bulk) CdTe; deconvolution of this rather broad (fwhm ~1.8 eV) set of bands yields two sets of bands separated by ~1 eV, the difference between Te^0 and Te^{2-} (Table II). Angularly resolved XPS data obtained by others[32] indicate that Te^0 and TeO_2 are present over similar electron escape depths. The layer of Te^0/TeO_2 found on CdTe treated with the oxidizing etch is not thick, as indicated by the presence and intensity of the Cd^{2+} and Te^{2-} 3d signals and the Te/Cd ratio of 1.6 (Table II). This contrasts the results of others, including researchers in this laboratory, who have found the same or similar oxidizing etches to give Te^0 and/or TeO_2 films thick enough to obscure the Cd signal.[1,34,35] This discrepancy is attributable to differences in time between etching and rinsing the samples.[36] Auger depth profile data indicate that the O signal falls off rapidly as the CdTe bulk is approached, suggesting a Te^0-rich layer in contact with bulk CdTe.[36]

The Te 3d spectrum for CdTe treated with the reducing etch, Figure 5, second from top, closely resembles that of sputter cleaned CdTe, third from top, implying that the

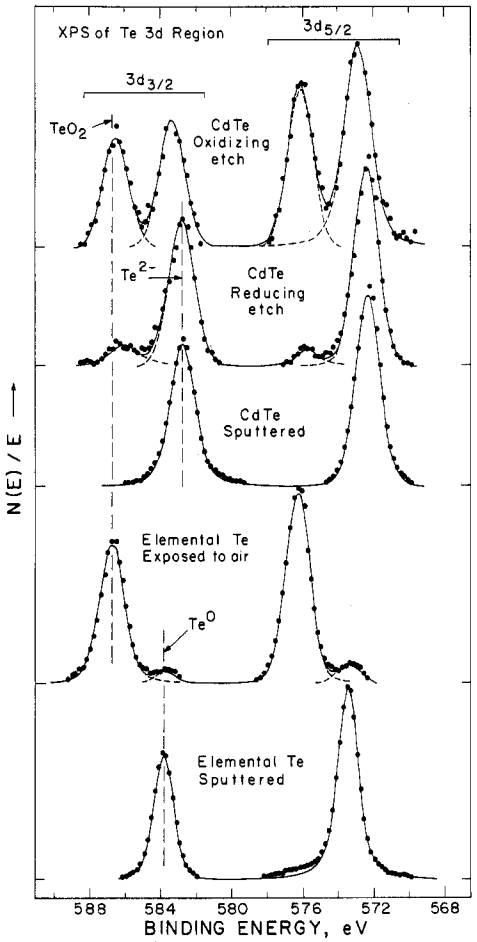

Figure 5. X-ray photoelectron spectra of the Te 3d region showing, from top: $HNO_3/Cr_2O_7^{2-}$-oxidized CdTe; $S_2O_4^{2-}/OH^-$-reduced CdTe; Ar-ion-sputtered CdTe; air-oxidized elemental Te; and Ar-ion-sputtered elemental Te.

reducing etch leaves a surface which resembles pure CdTe chemically; the difference in Te $3d_{5/2}$ binding energies is only 0.03 eV (Table II). The sputtered and reduced CdTe surfaces resemble one another stoichiometrically as well, both having a Cd/Te ratio of one (Table II). In addition to the predominant Te^{2-} peak, the spectrum of the reduced surface has a small, high-energy band attributable to TeO_2 from air oxidation of the surface;[37] the spectra of some reduced CdTe samples showed asymmetry on the high-

(30) Gaarenstroom, S. W.; Winograd, N. *J. Chem. Phys.* **1977**, *67*, 3500.
(31) Cotton, F. A.; Wilkinson, G. "Advanced Inorganic Chemistry", Wiley: New York, 1980; 4th ed, p 527.
(32) Patterson, M. H.; Williams, R. H. *J. Phys. D* **1978**, *11*, L83.
(33) Bahl, M. K.; Watson, R. L.; Irgolic, K. J. *J. Chem. Phys.* **1977**, *66*, 5526.
(34) (a) Zitter, R. N.; Charda, D. L. *J. Appl. Phys.* **1975**, *46*, 1405. (b) Zitter, R. N. *Surf. Sci.* **1971**, *28*, 335.
(35) Gaugash, P.; Milnes, A. G. *J. Electrochem. Soc.* **1981**, *128*, 924.
(36) Ricco, A. J.; White, H. S.; Wrighton, M. S. *J. Vac. Sci. Technol.*, submitted.
(37) Hage-Ali, M.; Stuck, R.; Saxena, A. N.; Siffert, P. *Appl. Phys.* **1979**, *19*, 25.

Scheme II: Representation of the CdTe/Te/TeO_2 Interfaces Resulting from an Oxidative Pretreatment of p-CdTe (left) and n-CdTe (right) Showing a Larger Barrier Height, $E_B = 0.8 \pm 0.1$ V, on n-CdTe than on p-CdTe, $E_B = 0.3 \pm 0.1$ V

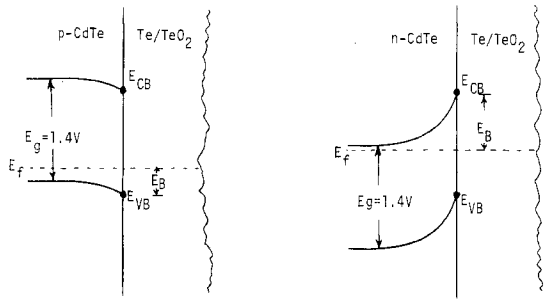

energy side of the Te^{2-} peak, suggesting the presence of a small amount of Te^0.

Sputtered-cleaned CdTe and Te^0 have X-ray photoelectron spectra containing only a single set of Te 3d bands (Figure 5), giving the 3d binding energies of Te^{2-} and Te^0, respectively (Table II). The spectrum of unsputtered (air oxidized) elemental Te (Figure 5, second from bottom) shows a small peak due to Te^0 and a much larger peak attributable to TeO_2,[33] indicating that Te^0 films formed on CdTe by an oxidizing etch are likely to be partially air-oxidized to TeO_2. In fact, allowing "reduced" CdTe samples to stand in air for ~2 weeks caused the small band attributed to TeO_2 to grow in intensity, indicating the Te^{2-} on the surface of CdTe is slowly air oxidized to TeO_2.[37]

The XPS studies indicate that the "oxidized" CdTe can be viewed as a situation where the bulk CdTe is coated with Te^0.[1,36] Thus, the space charge layer in the CdTe arises from the equilibration of CdTe with Te^0 just as for deliberately prepared heterojunctions such as CdTe/metal Schottky barriers. Interestingly, Te^0 is a large work function material[38] and would be expected, therefore, to give a larger barrier height on n-CdTe than on p-CdTe. We find tht the sum of the barrier heights for "oxidized" n- and p-CdTe is ~1.1 V, somewhat less than the 1.4-eV band gap would predict. However, the error in the values of E_B are at least ±0.1 V. Scheme II summarizes our view of the interface for "oxidized" CdTe where the space charge layer in the CdTe region is controlled by the Te^0/TeO_2 overlayer. The "reduced" CdTe behaves as a nearly ideal semiconductor[3,4] when in contact with electrolyte solutions. However, the photovoltage vs. E_{redox}, Figure 3, suggests recombination losses at the positive E_{redox} values, since there is significant curvature several tenths of a volt more negative than E_{FB}.

Photoelectrochemical Energy Conversion Using p-CdTe-Based Cells. The improvement in the ideality of n-CdTe using a reductive surface pretreatment cannot be easily exploited to improve the energy conversion efficiency for n-CdTe photoanode-based electrochemical cells. This is because the photoanodic decomposition of the surface of n-CdTe leads to rapid degradation of the improved barrier height, even though gross photocorrosion could likely be suppressed.[1] However, the improvement of p-CdTe could possibly be exploited, provided very negative redox couples are employed, Figure 3. Indeed, the capacitance measurements of "oxidized" p-CdTe held at a negative potential indicate that nearly ideal behavior can be induced by electrochemical reduction. Thus, p-CdTe could be protected from degradation under illumination

(38) Sze, S. M. "Physics of Semiconductor Devices"; Wiley: New York, 1981; 2nd ed, p, 251.

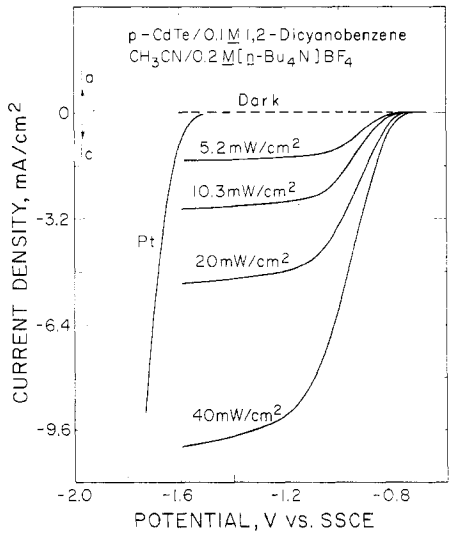

Figure 6. Steady-state photocurrent-potential curves for p-CdTe in CH_3CN/0.2 M $[n\text{-}Bu_4N]BF_4$ containing 0.1 M 1,2-dicyanobenzene. Electrodes were illuminated at 632.8 nm with a He-Ne laser at an input irradiation power as noted.

when electrons are driven to the surface. Accordingly, we have demonstrated that a p-CdTe-based photoelectrochemical cell can be efficient when using a sufficiently negative redox couple.

Figure 6 shows the steady-state photocurrent–voltage curves observed at "reduced" p-CdTe immersed in a 0.1 M 1,2-dicyanobenzene/CH_3CN/$[n\text{-}Bu_4N]BF_4$ solution. As expected from the cyclic voltammetric response, Figure 2, cathodic photocurrents are observed only when the electrode is irradiated. The onset of photocurrent begins at ~−0.8 V vs. SSCE which is ~0.7 V more positive than the onset of current at Pt. In essence, the reduction of 1,2-dicyanobenzene is driven at a light intensity limited rate at illuminated p-CdTe with a potential savings of ~0.7 V relative to its thermodynamic reduction potential. The quantum yield, fill factor, and power conversion efficiency at various light intensities are listed in Table III for three different photoelectrochemical cells, including one where the solution potential was poised by having a significant concentration of both halves of the redox couple. Interestingly, the photovoltage observed is up to 0.9 V, rivalling the best semiconductor photocathodes reported.[22] We note that the quantum yield for electron flow at short-circuit, Φ_e, is uncorrected for losses due to surface reflection which may be substantial on the shiny p-CdTe surfaces. However, Φ_e is large, ~0.6, and shows only a small decrease with increasing light intensity indicating that the photoresponse is not dominated by large recombination rates of electron–hole pairs at short circuit. The wavelength dependence of Φ_e shows an onset of photoresponse at E_g with a sharp rise at slightly higher energy, consistent with the fact that CdTe is a direct band-gap semiconductor.[13] The fill factor, which is a measure of the rectangularity of the photocurrent–voltage curves, is given by eq 6 where

$$\text{fill factor} = \frac{(iE_V)_{max}}{E_V(oc)i_{sc}} \tag{6}$$

$(iE_v)_{max}$ is the maximum power delivered by the photoelectrochemical cell. Values of the fill factor were in the range 0.4–0.5, decreasing with increasing light intensity. The maximum power conversion efficiency, η_{max}, given by eq 7 is ~8–10% for the reduction of the [1,2-dicyano-

$$\eta_{max} = \frac{(iE_V)_{max}}{\text{input power}} \times 100 \tag{7}$$

benzene]$^{0/-}$ system using 632.8-nm input optical energy.

The overall chemistry of this photoelectrochemical cell is given by

[1,2-dicyanobenzene]^0 + e$^-$ →
[1,2-dicyanobenzene]$^-$ (p-CdTe photocathode)

[1,2-dicyanobenzene]$^-$ →
[1,2-dicyanobenzene]^0 + e$^-$ (Pt counterelectrode)

The [1,2-dicyanobenzene]$^-$ photogenerated at p-CdTe is oxidized at the counterelectrode resulting in no net chemical change. The short-circuit current response under ~30 mW/cm^2 of 632.8-nm light slowly declines after about 1 h of operation. Although we have not investigated this instability in detail, loss of [1,2-dicyanobenzene]$^-$ occurs due to irreversible reactions with trace H_2O present in solution. The need to use very negative redox couples will likely be an impediment to practical photoelectrochemical energy conversion devices based on p-CdTe.

Conclusions

The photoelectrochemical behavior of p-CdTe immersed in electrolyte solutions has been shown to be strongly dependent on the nature of the surface pretreatment. As previously shown with n-CdTe photoanodes,[1] etching the photoelectrode with an oxidizing etch results in a constant photovoltage upon illumnation independent of the solution redox potential. This behavior has now been shown by XPS to result from a thin TeO_2/Te^0 surface layer which introduces a high density of surface levels capable of accumulating enough charge to shift the band edge positions with variation in E_{redox}. This situation is referred to as Fermi level pinning and dominates the behavior of p- or n-type CdTe etched by $Cr_2O_7^{2-}/HNO_3$ solutions. In contrast, p- and n-CdTe electrodes[1] etched by $S_2O_4^{2-}/OH^-$ behave in a more ideal fashion showing photovoltages that vary considerably with E_{redox}. Surface analysis reveals that the surface of such electrodes closely resembles bulk CdTe.

An important conclusion from these studies is that the barrier height of "oxidized" p- or n-type CdTe, as measured by the differential capacitance, agrees quite well with the value inferred from photovoltage determinations. This relationship is often assumed in photoelectrochemical studies[1,2,4,5] and the results presented here demonstrate its validity, at least in the case of CdTe photoelectrodes. Conventional electrochemical techniques, e.g., cyclic voltammetry, thus appear to be reliable means of mapping out the energetics of the semiconductor/electrolyte interface.

Modification of the p-CdTe surface by etching in $S_2O_4^{2-}/OH^-$ solutions has been demonstrated to yield relatively efficient photocathodes for the reduction of 1,2-dicyanobenzene. The visible light power conversion efficiency is considerably larger than previously reported[11] values for p-CdTe-based photoelectrochemical cells and represents the first efficient photoelectrochemical cell based on a p-type II–VI compound. We are presently extending these investigations to another II–VI semiconductor, p-ZnTe, which will be the subject of a future report. Finally, we note that work on CdTe/metal Schottky barriers has generally employed an oxidative pretreatment of the CdTe.[15,39] Our results indicate that different results could obtain for a reductive pretreatment. It is noteworthy that CdTe/metal Schottky barriers formed by in situ deposition of metals onto crystals of CdTe cleaved under vacuum show a strong dependence of E_B on metal work function,[40,41] whereas oxidatively pretreated CdTe yields an E_B that is less sensitive to the work function of the metal.[15,39]

Acknowledgment. This work was supported in part by the Office of Naval Research. Use of the Central Facilities of the M.I.T. Center for Materials Science and Engineering is grately acknowledged. A.J.R. acknowledges support as a NPW Predoctoral Fellow at M.I.T., 1982–1983.

Registry No. $Ru(bpy)_3^{2+}$, 15158-62-0; $Ru(bpy)_3^+$, 56977-24-3; $Ru(bpy)_3$, 74391-32-5; $Ru(bpy)_3^-$, 56977-23-2; $Cr_2O_7^{2-}$, 13907-47-6; CdTe, 1306-25-8; TeO_2, 7446-07-3; Te, 13494-80-9; HNO_3, 7697-37-2; $S_2O_4^{2-}$, 14844-07-6; OH^-, 14280-30-9; CH_3CN, 75-05-8; [*n*-Bu_4N]BF_4, 429-42-5; TCNQ, 1518-16-7; $TCNQ^-$, 34507-61-4; $TCNQ^{2-}$, 48161-40-6; MV^{2+}, 4685-14-7; MV^+, 25239-55-8; MV, 25128-26-1; BAQ, 84-47-9; BAQ^-, 77898-33-0; BAQ^{2-}, 84878-05-7; 1,2-DCB, 91-15-6; 1,2-DCB^-, 34536-45-3; An, 120-12-7; An^-, 34509-92-7.

(39) (a) Ponpon, J. P. *Appl. Phys. A* **1982**, *27*, 11, and references therein. (b) Anthony, T. C.; Fahrenbruch, A. L.; Bube, R. H. *J. Electron. Mater.* **1982**, *11*, 89.

(40) Takebe, T.; Saraie, J.; Tanaka, T. *Phys. Status Solidi A* **1978**, *47*, 123.

(41) (a) Humphreys, T. P.; Patterson, M. H.; Williams, R. H. *J. Vac. Sci. Technol.* **1980**, *17*, 886. (b) Patterson, M. H.; Williams, R. H. *Vacuum* **1981**, *31*, 639. (c) Williams, R. H.; Patterson, M. H. *Appl. Phys. Lett.* **1982**, *40*, 484.